Electronic Supplementary Material (ESI) for Journal of Materials Chemistry A.


# Supporting information

# For

# A-site Management and Oxygen-Deficient Regulation Strategy with Perovskite Oxide Electrocatalyst for Oxygen Evolution Reaction

Changhai Liu[a], Dingwei Ji[a], Hong Shi[c], Zhenyu Wu[c], Hui Huang[c,*], Zhenhui Kang[c,d], and Zhidong Chen[a,b,*],

[a]*School of Materials Science and Engineering, Jiangsu Key Laboratory of Materials Surface Science and Technology, Jiangsu Collaborative Innovation Center of Photovoltaic Science and Engineering, Changzhou University, Changzhou, 213164, Jiangsu, China.*

[b]*School of Petrochemical Engineering, Changzhou University, Changzhou, 213164, Jiangsu, China. E-mail: zdchen@cczu.edu.cn*

[c]*Institute of Functional Nano & Soft Materials (FUNSOM), Jiangsu Key Laboratory for Carbon-Based Functional Materials & Devices, Soochow University, 199 Ren'ai Road, Suzhou, 215123, Jiangsu, PR China. E-mail: hhuang0618@suda.edu.cn*

[d]*Macao Institute of Materials Science and Engineering, Macau University of Science and Technology, Taipa 999078, Macau SAR, China*

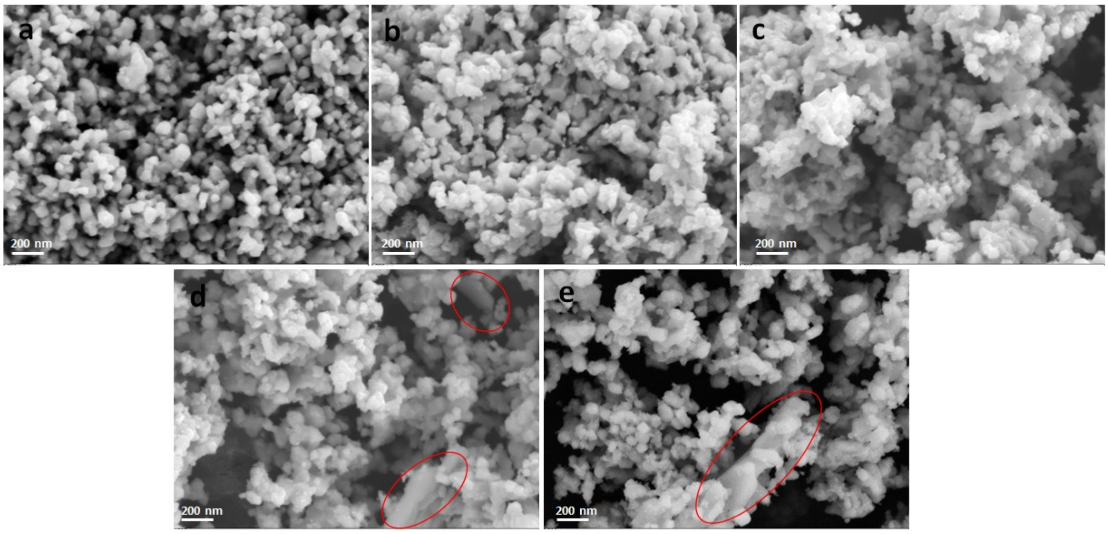


**Figure S1.** SEM images of a) $LaNiO_3$, b) LSN-0.05, c) LSN-0.15, d) LSN-0.1 (800°C), and e) LSN-0.1 (900°C).

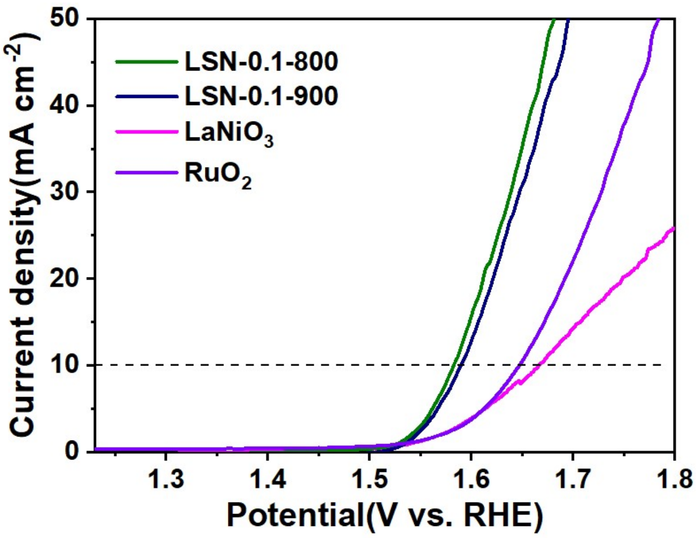


**Figure S2.** OER polarization curves of LSN-0.1-800, LSN-0.1-900, $LaNiO_3$, and $RuO_2$, in 0.1 M KOH solution.

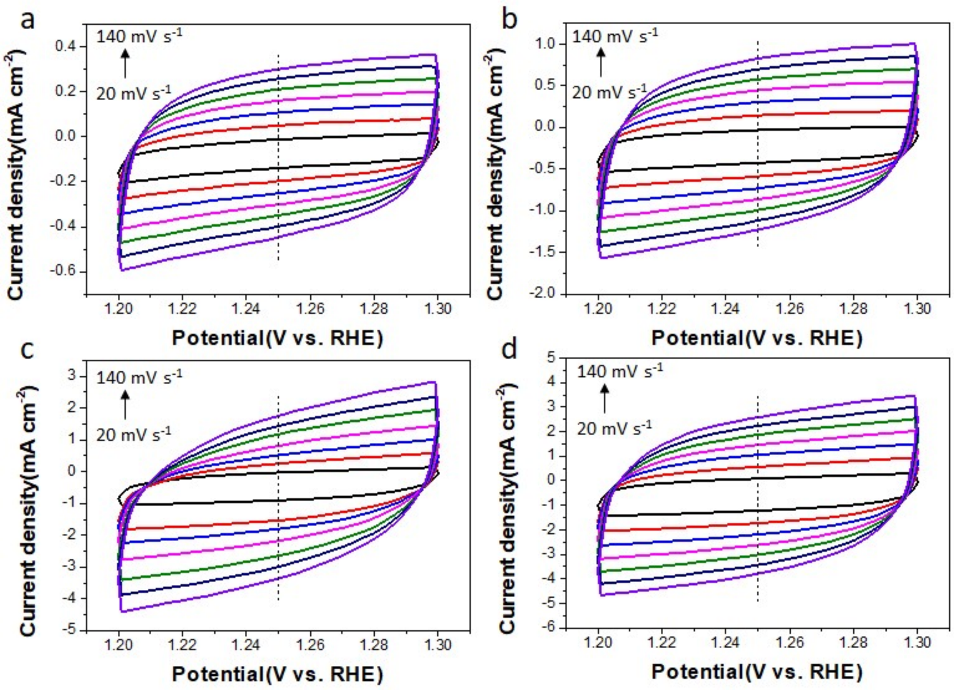


**Figure S3**. CV curves of a) LaNiO3, b) L0.85S0.05N, c) L0.85S0.15N, and d) L0.9S0.1N, respectively, with different scan rate from 20 to 140 mV.

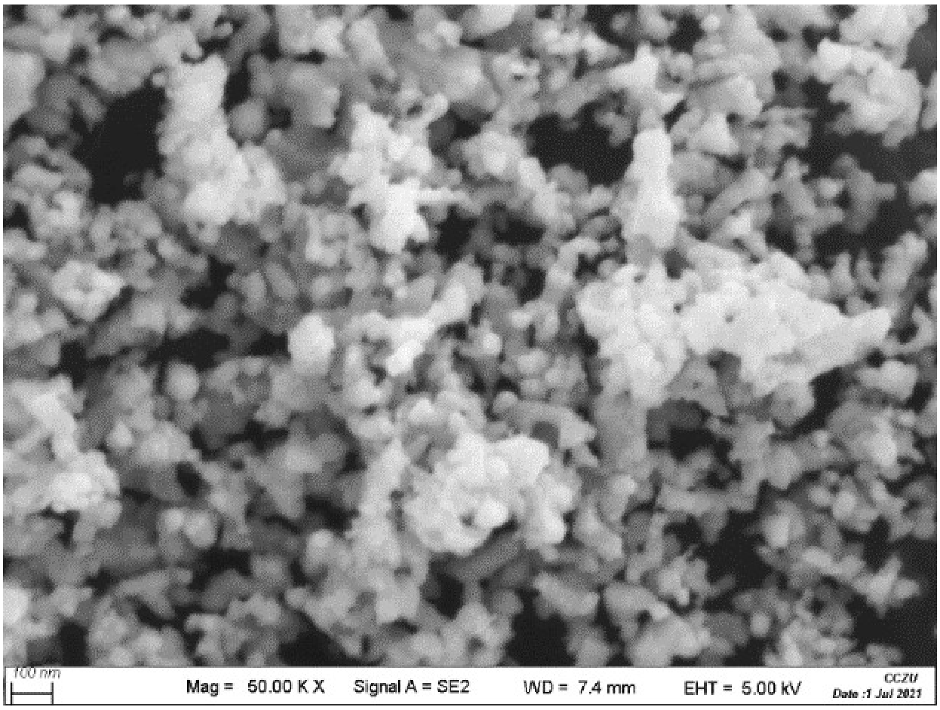


**Figure S4**. SEM image of L0.9S0.1N after long-term stability measurement.

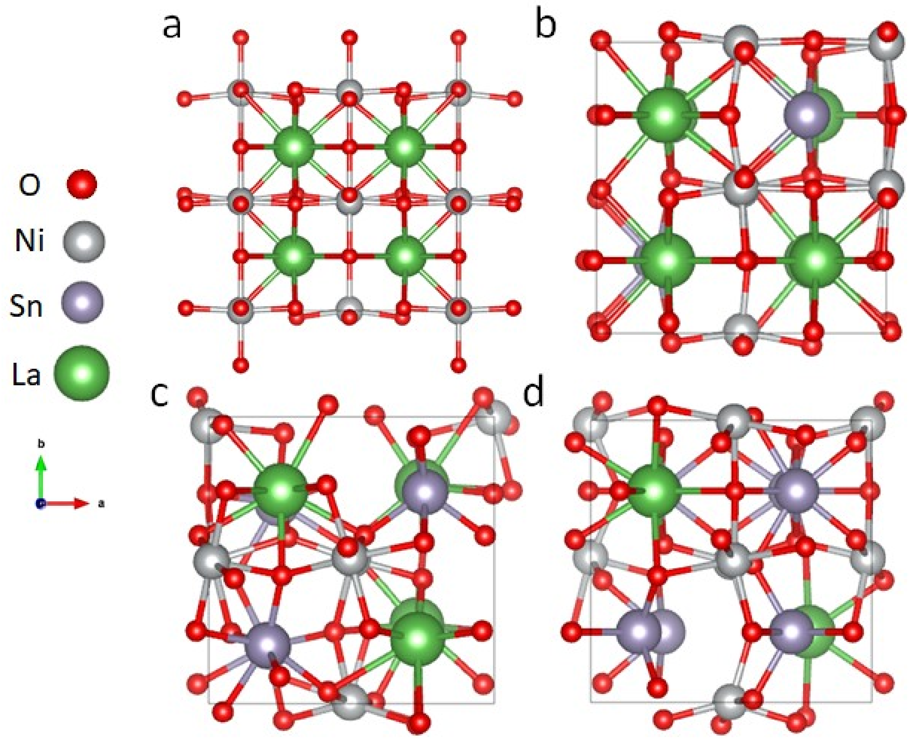


**Figure S5.** Calculation models of (a) $LaNiO_3$, (b) L0.95S0.05N, (c) L0.9S0.1N, and (d) L0.85S0.15N, respectively, with oxygen vacancy in the structure.

**Table S1**. Chemical composition of $La_{1-x}Sn_xNiO_{3-\delta}$ by ICP-AES analysis.

| Sample | La (mg $L^{-1}$) | Ni (mg $L^{-1}$) | Sn (mg $L^{-1}$) | Composition |
|---|---|---|---|---|
| **$LaNiO_3$** | 43.6 | 43.48 | ------ | $La_{1.003}NiO_3$ |
| **LSN-0.05** | 41.72 | 44.12 | 2.12 | $La_{0.946}Sn_{0.048}NiO_{3-\delta}$ |
| **LSN-0.1** | 45.28 | 50.60 | 4.8 | $La_{0.895}Sn_{0.095}NiO_{3-\delta}$ |
| **LSN-0.15** | 44.36 | 52.88 | 7.52 | $La_{0.839}Sn_{0.142}NiO_{3-\delta}$ |

**Table S2.** The binding energy (BE) and relative concentration of oxygen species from the deconvoluted O 1s XPS peaks.

| Perovskite electrocatalysts | | O 1s | | | | Area ratio |
|---|---|---|---|---|---|---|
| | | O1 | O2 | O3 | O4 | O2/(O1+O3+O4) |
| $LaNiO_3$ | Position [eV] | 528.6 | 529.5 | 531.4 | 532.4 | 0.042 |
| LSN-0.05 | Proportion [%] | 18.6 | 4.0 | 60.7 | 16.7 | |
| LSN-0.1 | Position [eV] | 528.6 | 529.5 | 531.4 | 532.4 | 0.140 |
| | Proportion [%] | 18.2 | 12.3 | 55.4 | 14.1 | |
| $LaNiO_3$ | Position [eV] | 528.4 | 529.5 | 531.4 | 532.4 | 0.197 |
| LSN-0.05 | Proportion [%] | 14.4 | 16.6 | 59.7 | 9.3 | |
| LSN-0.1 | Position [eV] | 528.65 | 529.5 | 531.3 | 532.4 | 0.187 |
| | Proportion [%] | 19.7 | 15.8 | 54.7 | 9.8 | |

**Table S3**. ESCA values under OER condition.

| Catalysts | C(F/g) | ECSA($m^2/g$) |
|---|---|---|
| $LaNiO_3$ | 2.67 | 4.45 |
| LSN-0.05 | 6.98 | 11.64 |
| LSN-0.1 | 21.46 | 35.77 |
| LSN-0.1&800 | 14.69 | 24.48 |
| LSN-0.1&900 | 12.63 | 21.01 |
| LSN-0.15 | 17.79 | 29.65 |

**Table S4**. The fitting parameters of EIS results

| | *$R_s$/Error* | *Q/Error* | *n/Error* | *$R_{CT}$/Error* |
|---|---|---|---|---|
| $LaNiO_3$ | 17.69,0.911 | 0.0001134,3.311 | 0.6752,0.9891 | 477.7,7.417 |
| LSN-0.05 | 18.40,1.250 | 0.0001921,4.244 | 0.6602,2.120 | 90.6,4.976 |
| LSN-0.1 | 17.78,1.051 | 0.0001494,14.729 | 0.6428,3.274 | 37.1,4.448 |
| LSN-0.15 | 18.87,0.914 | 0.0006348,5.755 | 0.7238,1.292 | 187.8,3.075 |

**Table S5.** Comparison of different perovskite-type oxides catalyst performance.

| Catalysts | OER performance ($mA/cm^2$) | OER Tafel slope(mV/dec) | References |
|---|---|---|---|
| $La_xSn_{1-x}NiO_3$ | 320 | 74 | *This work* |
| $La_xMnO_3$ | 419/ | 259 | Ref.1 |
| $La_xSr_{1-x}Co_yFe_{1-y}O_3$ | 360 | 77 | Ref.2 |
| $La_xSr_{1-x}CoO_3$ | 340 | 71 | Ref.3 |
| $La_xCoO_3$ | 380 | 83 | Ref.4 |
| $La_xCe_{1-x}CoO_3$ | 430 | 112 | Ref.5 |
| $La_{1-x}CoO_3$ | 380 | 83 | Ref.6 |
| $Pr_{0.5}Ba_{0.5}Mn_{1.8-x}Nb_xCo_{0.2}O_{6-\delta}$ | 370 | 109 | Ref.7 |
| $BaPrMn_{2-x}Co_xO_{5+\delta}$ | 430 | 102 | Ref.8 |
| $La_{0.8}Sr_{0.2}Mn_{1-x}Co_xO_3$ | 439 | 133 | Ref.9 |
| $La_{0.6}Sr_{0.4}CoO_{3-\delta}$ | 421 | 123 | Ref.10 |
| $(La_{0.8}Sr_{0.2})_{1-x}MnO_3$ | 540 | 326 | Ref.11 |
| $La_{0.6}Sr_{0.4}CoO_{3-\delta}$ | 400 | 105 | Ref.12 |

**References**:

1. G. S. Hegde, A. Ghosh, R. Badam, N. Matusmi and R. Sundara, *ACS Appl. Energy Mater*., 2020, **3**, 135566.
2. W. Guo, L. Cui, H. W. Xu and C. R. Gong, *Appl. Surf. Sci*., 2020, **529**, 147165.
3. Y. Lu, A. J. Ma, Y. F. Yu, R. Tan, C. W. Liu, P. Zhang, D. Liu and J. Z. Gui, *ACS Sustainable Chem. Eng*., 2019, **7**, 2906-2910.
4. H. Z. Wang, X. Q. Chen, D. Huang, M. Zhou, D. Ding and H. M. Luo, *ChemCatChem,* 2020, **12**, 2768-2775.
5. J. M. Qian, T. T. Wang, Z. M. Zhang, Y. G. Liu, J. F. Li and D. Q. Gao, Nano Energy, 2020, 74, 104948.
6. H. Z. Wang, X. Q. Chen, D. Huang, M. Zhou, D. Ding and H. M. Luo, *ChemCatChem*, 2020, **12**, 2768-2775.
7. S. Mondal, R. Majee, Q. A. Islam and S. Bhattacharyya, *ChemCatChem*, 2020, **7**, 5005-5012.
8. R. Majee, Q. A. Islam, S. Mondal and S. Bhattacharyya, *Chem. Sci*., **2020**, 11, 10180-10189.
9. C. H. Li, J. S. Cheng, Y. Jiang, W. Xiao and X. M. Yan, *J. Power Sources*, 2021, **498**, 229940.
10. O. Miyeong, L. Jongju, P. Hyoseok, T. K. Young, Y. S. Lee, V. Aravindan and N. Giseok, *J. Ind. Eng. Chem*., 2019, **80**, 686-689.
11. R. H. Yuan, Y. He, W. He, M. Ni and M. Leung, *Appl. Energy*, 2019, **251**, 113406.
12. V. F. Mattick, X. F. Jin, R. E. White and K. Huang, *J. Electrochem. Energy Convers*. *Storage*, 2019, 23, 537-543.